HIGH-ORDER MOMENT SCALING OF NEAR-WALL TURBULENCE FOR ARBITRARY VELOCITIES: AN EXTENDED SYMMETRY THEORY

Martin Oberlack, Simon Görtz, Paul Hollmann and Johannes Conrad
Chair of Fluid Dynamics, Technical University of Darmstadt
Otto-Bernd-Straße 2, 64287 Darmstadt, Germany
Centre for Computational Engineering, TU Darmstadt
Dolivostrasse 15, 64293 Darmstadt, Germany
oberlack@fdy.tu-darmstadt.de

Sergio Hoyas
Instituto Universitario de Matemática Pura y Aplicada, UP València
Camino de Vera, 46024 València, Spain

ABSTRACT

Based on symmetry theory of the infinite multi-point moment hierarchy and standard physical constraints, scaling laws for log and center regions of a turbulent channel flow were derived for the mean velocity first in [Oberlack, JFM 427, 299 (2001)], and significantly expanded to higher moments of the streamwise velocity U_1 in [Oberlack et al., PRL 128, 024502 (2022)]. We presently further extend the theory to arbitrary velocity moments, in which U_2 and U_3 do not contain the mean. Direct numerical simulations at $Re_\tau = 10^4$, performed with extended integration time, show excellent agreement with the theoretical predictions for all moments considered. A central result is that the scaling exponents in the log and center regions are identical for all velocity moments, demonstrating a previously unrecognized universality in turbulent wall-bounded flows. These scaling laws are shown to arise as invariant solutions of the infinite hierarchy of multi-point moment equations, with all the theoretical development explained in an extended theoretical paper [Görtz et al., PRF, (2026)].

1 INTRODUCTION

Osborne Reynolds Reynolds (1895) was the first to realize that the statistical description of turbulence leads to an infinite system of moment equations. The single-point hierarchy generates several new unclosed terms at every order, a problem partially overcome by the multi-point moment hierarchies of Keller & Friedmann L. Keller & A. Friedmann (1924). Therein, only one term per level is unclosed at the price of three extra dimensions per order, leading to an infinite-dimensional system.

Over a century of turbulence research has dealt with this "curse of dimensions" in many ways. Scaling laws gained early acceptance, either via dimensional reasoning Kolmogorov (1941) or via a finite number of moment equations, starting with Kármán and Howarth's similarity solution of the two-point isotropic equation von Kármán & Howarth (1938).

For wall-bounded shear flows, the log law was originally derived from the eddy-viscosity hypothesis von Kármán (1930); L. Prandtl (1932) and has since been revisited by many authors Isakson (1937); Millikan (1938); Clauser (1954); Coles (1956); George (2006); Klewicki *et al.* (2009).

A first attempt to derive the log law from the Navier-Stokes equations, their symmetries, and the resulting statistical equations was made in Oberlack (2001), though limited to the mean velocity. In Oberlack & Rosteck (2010), statistical symmetries were discovered that are not apparent in the Navier-Stokes equations alone but were proven for the infinite multi-point moment hierarchy; their interpretation as intermittency and non-Gaussianity followed in Wacławczyk *et al.* (2014). These classical and statistical symmetries were the starting point for the U_1-moment scaling laws of Oberlack *et al.* (2022), substantiated by DNS for the log and the centre region of plane Poiseuille flow.

The present and the extended theoretical paper Görtz *et al.* (2026) expands this development in two directions: we generalise the scaling laws to arbitrary multi-point moments substantiated by DNS data up to order six, and Görtz *et al.* (2026) establishes that these scaling laws are similarity solutions of the infinite multi-point moment hierarchy.

2 BASIC EQUATION

Starting point are the Navier-Stokes equations

$$\frac{\partial U_i}{\partial t} + U_k \frac{\partial U_i}{\partial x_k} + \frac{\partial P}{\partial x_i} - \nu \frac{\partial^2 U_i}{\partial x_k \partial x_k} = 0\,, \quad \frac{\partial U_k}{\partial x_k} = 0, \qquad (1)$$

with $t \in \mathbb{R}^+$, $\boldsymbol{x} \in \mathbb{R}^3$, $\boldsymbol{U} = \boldsymbol{U}(\boldsymbol{x},t)$, $P = P(\boldsymbol{x},t)$, and ν representing time, position vector, instantaneous velocity vector, pressure, and kinematic viscosity, respectively. Rather different to the common Reynolds' decomposition, i.e. $U_k = \bar{U}_k + u_k$, where $\bar{U}_k$ and u_k are, respectively, mean and fluctuation, we presently adopt an alternative approach by utilizing statistical moments encompassing the full instantaneous velocities instead of the fluctuations only. Consequently, the generic multipoint velocity moments read

$$H_{i_{\{n\}}} = H_{i_{(1)}\dots i_{(n)}} = \overline{U_{i_{(1)}}(\boldsymbol{x}_{(1)},t)\cdot\ldots\cdot U_{i_{(n)}}(\boldsymbol{x}_{(n)},t)}\,. \qquad (2)$$

As in Oberlack *et al.* (2022) (for details see the extended theoretical publication Görtz *et al.* (2026)), the multipoint moment equation (MPME) for the velocity yields

$$\frac{\partial H_{i_{\{n\}}}}{\partial t}+\sum_{l=1}^{n}\left[\frac{\partial H_{i_{\{n+1\}}[i_{(n)}\mapsto k_{(l)}]}[\boldsymbol{x}_{(n)}\mapsto\boldsymbol{x}_{(l)}]}{\partial x_{k_{(l)}}}\right.$$
$$\left.+\frac{\partial I_{i_{\{n-1\}}[l]}}{\partial x_{i_{(l)}}}-\nu\frac{\partial^2 H_{i_{\{n\}}}}{\partial x_{k_{(l)}}\partial x_{k_{(l)}}}\right]=0. \qquad (3)$$

The moment $I_{i_{\{n-1\}}[l]}$ correlates the pressure with $n-1$ velocities (see e.g. Oberlack & Rosteck (2010)).

Definition (2) and the infinite-dimensional system (3) form the foundation of symmetry-based turbulence theory, which is presented in depth in the extended theoretical paper Görtz *et al.* (2026). Presently, an abbreviated theory is presented for comparison with the DNS data, and, hence, we focus on one-point statistics, i.e., $\boldsymbol{x}=\boldsymbol{x}_{(1)}=\boldsymbol{x}_{(2)}=\ldots=\boldsymbol{x}_{(n)}$, for which we introduce the classical notation $\overline{U_1^iU_2^jU_3^k}$ with $i,j,k\in\mathbb{N}_0$.

We note that working with instantaneous rather than fluctuating moments is not a loss of generality: the symmetry structure of the instantaneous hierarchy (3) is fully equivalent to that of the fluctuation hierarchy obtained via Reynolds decomposition, since Lie symmetries are preserved under such invertible linear transformations; this equivalence is made explicit in Sec. V of Görtz *et al.* (2026).

3 LIE SYMMETRIES AND INVARIANT SOLUTIONS

Very briefly, let us define the idea of a form-invariant transformation $\boldsymbol{x}^*=\boldsymbol{\phi}(\boldsymbol{x},\boldsymbol{y};a)$, $\boldsymbol{y}^*=\boldsymbol{\psi}(\boldsymbol{x},\boldsymbol{y};a)$, also called a Lie symmetry transformation, which leaves a differential equation $\boldsymbol{F}=0$ unchanged so that holds

$$\boldsymbol{F}\left(\boldsymbol{x},\boldsymbol{y},\boldsymbol{y}^{(1)},\boldsymbol{y}^{(2)},\ldots,\boldsymbol{y}^{(p)}\right)=0$$
$$\Leftrightarrow\quad \boldsymbol{F}\left(\boldsymbol{x}^*,\boldsymbol{y}^*,\boldsymbol{y}^{*(1)},\boldsymbol{y}^{*(2)},\ldots,\boldsymbol{y}^{*(p)}\right)=0, \qquad (4)$$

with the p^{th} derivatives of $\boldsymbol{y}$ defined as $\boldsymbol{y}^{(p)}$.

The symmetries of the system (3) known so far are divided into (i) those inherited from the Navier-Stokes equations (1) to (3) and (ii) those found only in (3) and, therefore, called statistical symmetries.

Of the nine symmetries of the Navier-Stokes equations (1), only the combined space-time scaling symmetry

$$T_{Sx/St}:\ t^*=\mathrm{e}^{a_{St}}t,\ \ \boldsymbol{x}^*=\mathrm{e}^{a_{Sx}}\boldsymbol{x},$$
$$\boldsymbol{U}^*=\mathrm{e}^{a_{Sx}-a_{St}}\boldsymbol{U},\ \ P^*=\mathrm{e}^{2(a_{Sx}-a_{St})}P, \qquad (5)$$

for the case of vanishing viscosity and the translation symmetry in space are subsequently employed,

$$T_{x_i}:\ \ t^*=t,\ \ \boldsymbol{x}^*=\boldsymbol{x}+\boldsymbol{a_x},\ \ \boldsymbol{U}^*=\boldsymbol{U},\ \ P^*=P. \qquad (6)$$

In the moment frame, the scaling symmetries (5) read

$$\bar{T}_{Sx/St}:\ t^*=\mathrm{e}^{a_{St}}t,\ \ \boldsymbol{x}^*_{(i)}=\mathrm{e}^{a_{Sx}}\boldsymbol{x}_{(i)},$$
$$\bar{\boldsymbol{U}}^*=\mathrm{e}^{a_{Sx}-a_{St}}\bar{\boldsymbol{U}}^*,\mathbf{H}^*_{\{n\}}=\mathrm{e}^{n(a_{Sx}-a_{St})}\mathbf{H}_{\{n\}}, \qquad (7)$$

and the translation symmetry turns into

$$\bar{T}_{x_i}:t^*=t,\boldsymbol{x}^*_{(i)}=\boldsymbol{x}_{(i)}+\boldsymbol{a_x},\bar{\boldsymbol{U}}^*=\bar{\boldsymbol{U}}^*,\ \mathbf{H}^*_{\{n\}}=\mathbf{H}_{\{n\}}. \qquad (8)$$

The proof of form invariance is easily obtained by substituting (7) and (8) into (3).

A subtlety arises from the viscous term: the Navier-Stokes equation (1) admits only one scaling symmetry, whereas the Euler equation and the inviscid MPME (3) with $\nu=0$ admit two, cf. (5) and (7). This apparent contradiction is resolved by a singular asymptotic expansion in the Kolmogorov scale η as the perturbation parameter – a boundary-layer-type decomposition of the MPME in separation space $\boldsymbol{r}$. This was first introduced in Oberlack & Peters (1993) for isotropic turbulence, and gained widespread recognition thanks to Lundgren's famous work Lundgren (2003). Extended to the present hierarchy for arbitrary turbulent shear flows is presented in full detail in Sec. II B of Görtz *et al.* (2026). The expansion yields two equations: an outer equation on scales, which is simply (3) with $\nu=0$, which hold into the inertial subrange for $\eta\ll|\boldsymbol{r}|$, and governs the log and centre regions, and an inner equation on scales $|\boldsymbol{r}|\sim\eta$ where viscosity is dominant. All scaling laws derived below follow from the outer, viscosity-free system.

The statistical symmetries mentioned above under point (ii) were first derived in Oberlack & Rosteck (2010) and in Wacławczyk *et al.* (2014) their physical meaning was pointed out. The translation symmetry in the moments

$$\bar{T}'_{\{n\}}:\ t^*=t,\ \ \boldsymbol{x}^*_{(i)}=\boldsymbol{x}_{(i)},$$
$$\bar{\boldsymbol{U}}^*=\bar{\boldsymbol{U}}+\boldsymbol{a},\ \ \mathbf{H}^*_{\{n\}}=\mathbf{H}_{\{n\}}+\mathbf{a}^H_{\{n\}} \qquad (9)$$

refers to non-gaussianity. The statistical scaling symmetry in the moments

$$\bar{T}'_s:\ t^*=t,\ \ \boldsymbol{x}^*_{(i)}=\boldsymbol{x}_{(i)},$$
$$\bar{\boldsymbol{U}}^*=\mathrm{e}^{a_{Ss}}\bar{\boldsymbol{U}},\ \ \mathbf{H}^*_{\{n\}}=\mathrm{e}^{a_{Ss}}\mathbf{H}_{\{n\}}, \qquad (10)$$

can be traced back to intermittency and has its causes in the linearity of the infinite system (3).

Finally, the MPME (3) admits symmetries limited to plane shear flows, with x_2 the wall-normal coordinate

$$\bar{T}'_L:\ t^*=t,\ \ \boldsymbol{x}^*_{(i)}=\boldsymbol{x}_{(i)},$$
$$\bar{\boldsymbol{U}}^*=\bar{\boldsymbol{U}}+x_2\boldsymbol{a}^L_{\{1\}},\ \ \mathbf{H}^*_{\{n\}}=\mathbf{H}_{\{n\}}+x_2\mathbf{a}^L_{\{n\}}, \qquad (11)$$

This symmetry has already been discovered in Rosteck (2013) and, as we will see later, leads to a linear adjustment of the scaling laws in the log region. For the center region, this symmetry is meaningless, as it would break the reflection symmetry of the channel. The linear correction was already analyzed by us in Oberlack *et al.* (2022) for the U_1 scaling laws, but the DNS data induced an extremely small prefactor, so the term was not listed. We see later that the prefactor of the linear term is also very small for most of the moments, but by no means negligible.

The form invariance of the MPME (3) under the statistical symmetries (9)–(11) can be verified by direct substitution: inserting, e.g., $\mathbf{H}^*_{\{n\}}=\mathbf{H}_{\{n\}}+\mathbf{a}^H_{\{n\}}$ from (9) into (3) leaves every term unchanged, since (3) is linear in $\mathbf{H}_{\{n\}}$ and contains only derivatives with respect to $\boldsymbol{x}_{(i)}$ and t, while $\mathbf{a}^H_{\{n\}}$ is a constant with respect to these variables. Form invariance therefore holds at the level of the equations themselves and requires, for the present purpose, no additional closure hypothesis.

With this, invariant solutions for $\overline{U_1^iU_2^jU_3^k}$ are derived from the aforementioned symmetries rather similar to $\overline{U_1^n}$ in Oberlack *et al.* (2022). Also here, we restrict ourselves to one-point statistics in comparison with the DNS data, but in the extended theoretical article Görtz *et al.* (2026), the complete invariant solution for arbitrary multi-point moments $\mathbf{H}_{\{n\}}$ is generated and, moreover, the symmetry or similarity reduction of the MPME (3) is proven in Sec. IV C therein, showing that the scaling laws reduce the number of independent variables in (3) – the defining property of an invariant solution in the Lie-group sense. With this, the characteristic system for the invariant solution of arbitrary one-point velocity moments reads,

$$\frac{\mathrm{d}x_2}{a_{Sx}x_2+a_{x_2}} = \frac{\mathrm{d}\overline{U}_1}{[a_{Sx}-a_{St}+a_{Ss}]\overline{U_1}+a^H_{[1,0,0]}+x_2a^L_{[1,0,0]}} = \dots = \frac{\mathrm{d}\overline{U_1^iU_2^jU_3^k}}{[n(a_{Sx}-a_{St})+a_{Ss}]\overline{U_1^iU_2^jU_3^k}+a^H_{[i,j,k]}+x_2a^L_{[i,j,k]}}. \quad (12)$$

Here and in the following, only the notation $\overline{U_1^iU_2^jU_3^k}$ is used, we recall $i,j,k\in\mathbb{N}_0$, and introduce the abbreviation $n=i+j+k$, and a_{Sx}, a_{St}, a_{Ss} are scaling group parameters. It may appear surprising that the infinitely many equations of (3) admit, simultaneously, only a finite set of three scaling groups with the parameters $\{a_{Sx},a_{St},a_{Ss}\}$. a_{Ss} is a consequence of the linearity of (3) across *all* moments and a_{Sx},a_{St} of the scaling of space and time in (7). The boundary information specific to each moment is, in turn, encoded in the integration constants in (19), (20) and (21), see Görtz *et al.* (2026) for the full argument. For the sake of completeness, we have included the mean velocity in (12), though it is not to be compared to DNS data. Combining the scaling groups (7) and (10), we obtain

$$\bar{T}_{Scale}:\; x_2^*=\mathrm{e}^{a_{Sx}}x_2,\;\; \overline{U_1}^*=\mathrm{e}^{a_{Sx}-a_{St}+a_{Ss}}\overline{U_1},$$
$$\overline{U_1^iU_2^jU_3^k}^*=\mathrm{e}^{n(a_{Sx}-a_{St})+a_{Ss}}\overline{U_1^iU_2^jU_3^k}. \quad (13)$$

4 TURBULENT WALL-BOUNDED SCALING LAWS

In the context of integrating (12), we need to distinguish two cases, i.e. the solutions corresponding to the log and centre regions of the channel (see (Oberlack *et al.*, 2022)). The pivotal parameter governing the log-law is the wall shear stress velocity denoted as $u_\tau=\sqrt{\tau_w/\rho}$, where τ_w denotes the wall shear stress, and ρ represents density. u_τ serves as the exclusive near-wall velocity scale. Consequently, this means that scaling the mean velocity in equation (13) is no longer permissible, and results in a symmetry breaking of the velocity scaling, i.e.

$$a_{Sx}-a_{St}+a_{Ss}=0. \quad (14)$$

If we use this symmetry-breaking equation in (12) and integrate, we find

$$\bar{U}_1=\frac{a^H_{[1,0,0]}a_{Sx}-a^L_{[1,0,0]}a_{x_2}}{a^2_{Sx}}\ln\left(x_2+\frac{a_{x_2}}{a_{Sx}}\right)+\frac{a^L_{[1,0,0]}}{a_{Sx}}x_2+\tilde{C}_1, \quad (15)$$

and

$$\overline{U_1^iU_2^jU_3^k}=\tilde{C}_{[i,j,k]}\left(x_2+\frac{a_{x_2}}{a_{Sx}}\right)^{\omega(n-1)}-\frac{a^H_{[i,j,k]}(1-\omega(n-1))-a^L_{[i,j,k]}\frac{a_{x_2}}{a_{Sx}}}{a_{Sx}\omega(n-1)(1-\omega(n-1))}+\frac{a^L_{[i,j,k]}}{a_{Sx}(1-\omega(n-1))}x_2, \quad (16)$$

where, as already mentioned above, in Oberlack *et al.* (2022) all $a^L_{[i,0,0]}$ in the data proved to be very small and were neglected during DNS data fitting. The moments $\overline{U_1^i}$ in (15) and (16) then reduce to the results in Oberlack *et al.* (2022). Further, $\omega=1-a_{St}/a_{Sx}$ is a universal constant, and $\tilde{C}_{[i,j,k]}$ denote constants of integration. In particular, also in comparison with the log region for the U_1 moments in Oberlack *et al.* (2022) we find five key results: (i) moments $n=i+j+k\geq 2$ have a power law relationship, (ii) the exponent ω links arbitrary moments, (iii) the power law behaves identically for all three U_i components, and the current DNS data clearly prove this to be shown below, and (iv) in connection with Görtz *et al.* (2026), we find that the above scaling laws are invariant solutions of the infinite hierarchy of moment equations.

As already shown in Oberlack *et al.* (2022), the second case led to deficit type of power laws for $\overline{U_1^i}$ in the channel center. For this, it is assumed that none of the scaling factors in (12) and (13) vanish, i.e. $(a_{Sx}-a_{St}+a_{Ss})\neq 0,\dots,n(a_{Sx}-a_{St})+a_{Ss}\neq 0$. Due to the reflection symmetry, in this case we have $a^L_{[i,j,k]}=0$, and after integrating (12), we find

$$\overline{U_1^iU_2^jU_3^k}=\tilde{C}'_{[i,j,k]}\left(x_2+\frac{a_{x_2}}{a_{Sx}}\right)^{n(\sigma_2-\sigma_1)+2\sigma_1-\sigma_2}-\frac{a^H_{[i,j,k]}}{n(a_{Sx}-a_{St})+a_{Ss}}, \quad (17)$$

where

$$\sigma_1=1-\frac{a_{St}}{a_{Sx}}+\frac{a_{Ss}}{a_{Sx}},\;\; \sigma_2=2\left(1-\frac{a_{St}}{a_{Sx}}\right)+\frac{a_{Ss}}{a_{Sx}} \quad (18)$$

are known exponents from Oberlack *et al.* (2022), $n=i+j+k$, and the $\tilde{C}'_{[i,j,k]}$ are constants of integration. We will see below from DNS data that σ_1 and σ_2 are universal constants across all moments. For both of the above scaling laws (16) and (18), we found in Oberlack *et al.* (2022) for the U_1-moments that the factors $\tilde{C}_{[i,j,k]}$ and $\tilde{C}'_{[i,j,k]}$ are exponential functions of the moment order. This result can only be extended to other moments to a limited extent, so it will not be considered here.

To improve the statistics for comparison with the above scaling laws, we extended the DNS of Oberlack *et al.* (2022); Hoyas *et al.* (2022) and doubled the integration time to 100 million CPU-hours, keeping all other parameters unchanged at $Re_\tau=10^4$. The extension was particularly necessary for the U_2 and U_3 statistics, whose convergence is poorer than for U_1 due to the absence of a mean.

Even with improved statistics, convergence deteriorates with moment order and we restrict ourselves to order 6, as in Oberlack *et al.* (2022). Odd moments in U_2 and U_3 are exactly zero by reflection symmetry and were excluded; moments of order 5 were excluded for convergence reasons; some sixth-order moments were also excluded for the same reason. The retained moments used for the comparison are: $\bar{U}_1$, $\overline{U_1^2}$, $\overline{U_2^2}$, $\overline{U_3^2}$, $\overline{U_1^3}$, $\overline{U_1U_2^2}$, $\overline{U_1U_3^2}$, $\overline{U_1^4}$, $\overline{U_2^4}$, $\overline{U_3^4}$, $\overline{U_1^2U_2^2}$, $\overline{U_1^2U_3^2}$, $\overline{U_2^2U_3^2}$, $\overline{U_1^6}$, $\overline{U_2^6}$, $\overline{U_3^6}$, $\overline{U_1^4U_2^2}$, $\overline{U_1^4U_3^2}$, $\overline{U_2^4U_1^2}$, $\overline{U_2^4U_3^2}$, $\overline{U_3^4U_1^2}$, $\overline{U_3^4U_2^2}$, and $\overline{U_1^2U_2^2U_3^2}$.

For comparison with the DNS data, the extended scaling laws derived above are now rewritten using the nomenclature common in the turbulence community. Equations (15) and (16) then become

$$\bar{U}_1^+=\frac{1}{\kappa}\ln\left(y^+\right)+B+Dy^+, \quad (19)$$
$$\overline{U_1^iU_2^jU_3^k}^+=C_{[i,j,k]}\left(y^+\right)^{\omega(n-1)}-B_{[i,j,k]}+D_{[i,j,k]}y^+,\quad \text{for } n=i+j+k\geq 2, \quad (20)$$

where $y^+=yu_\tau/\nu$, $\overline{U_1^iU_2^jU_3^k}^+=\overline{U_1^iU_2^jU_3^k}/u_\tau^n$, and $y^+=0$ denotes the wall. The parameters B, D, $B_{[i,j,k]}$, $C_{[i,j,k]}$, $D_{[i,j,k]}$,

α, β, $\tilde{\alpha}$, $\tilde{\beta}$ and von Kármán's constant κ contain the group parameters appearing in Eq. (15) and (16).

The log law (19) will not be considered further, because $\kappa = 0.394$ from Oberlack *et al.* (2022) remains unchanged, and D is still negligibly small. Furthermore, as in Oberlack *et al.* (2022), the shift in y^+ will also be neglected here, i.e., $a_{x_2} = 0$ in Eqs. (15) and (16).

For a consistent comparison with the theory in Görtz *et al.* (2026), the value of ω must be identical for all moments. Currently, we have adopted the value of $\omega = 0.1$ from Oberlack *et al.* (2022), which continues to be the optimal choice here as well. We emphasise that the functional form of (20), the universality of ω across moments and components, and the fact that a single exponent governs all $n \geq 2$ are predictions of the symmetry analysis; the numerical value $\omega \approx 0.10$ itself is an empirical input, fitted from the DNS, in the same spirit in which von Kármán's constant κ is fitted from data.

The first key result here is the comparison of the moments $n \geq 2$ taken from the DNS data with the scaling law (20) in the fitting window $y^+ \simeq 400 \ldots 2500$ also chosen in Oberlack *et al.* (2022). The corresponding results are shown on a double-logarithmic scale, and the universal value $\omega = 0.1$ from Oberlack *et al.* (2022) was used, which is also here the optimal value. The comparisons are divided into four subimages of figure 1, each of which shows the moments of order 2, 3, 4, and 6 listed above. In all cases, the data show extremely good agreement with the scaling laws (20); the residual deviation of the fitted from the theoretical exponents stays below approximately 1% across all moments considered. Some fitted curves follow the DNS data even to $y^+ \approx 100$. Still, we restrict the fitting itself to $y^+ \simeq 400 \ldots 2500$, to ensure consistency and a minimal error for all moments, and since below this range buffer-layer dynamics may become non-negligible. The corresponding data for the parameters in equation (20) are taken from Oberlack & Hoyas (2026). For the second-order wall-normal moment, the prefactor $C_{[0,2,0]}$ in (20) is of the same order of magnitude as the asymptotic high-Reynolds-number value $\overline{U_2^2}^+ \to 1.3$ reported in Örlü *et al.* (2017); Spalart & Abe (2021). For the spanwise variance $\overline{U_3^2}$, the attached-eddy hypothesis of Townsend Townsend (1976) (see also Marusic & Monty (2019)) predicts a $\ln(y/h)$ profile; this is consistent with (20) for $n = 2$, since the present power law with the small exponent $\omega(n-1) = \omega \approx 0.10$ is numerically nearly indistinguishable from a logarithm over the observed log range, while sharpening Townsend's statement by predicting a small but universal positive exponent rather than zero.

A second fundamental result links the present verification of the scaling laws to the theoretical proof that generalizing the single-point moments (19) to multi-point moments exactly satisfies the infinite multi-point moment equation Görtz *et al.* (2026). Inserting the scaling laws reveals a symmetry reduction, similar to the Blasius solution — shown here for the first time for an infinite-dimensional system.

The second region, the channel center, which was analyzed in Oberlack *et al.* (2022) for U_1-moments only, shall also be reconsidered here in much greater generality. For this case, $x_2 = 0$ refers to the channel center, which also represents the symmetry axis for all moments. Although most moments are reflection symmetric, those odd in U_2 are point symmetric. For this reason, symmetry (11) has already been omitted in (17) a

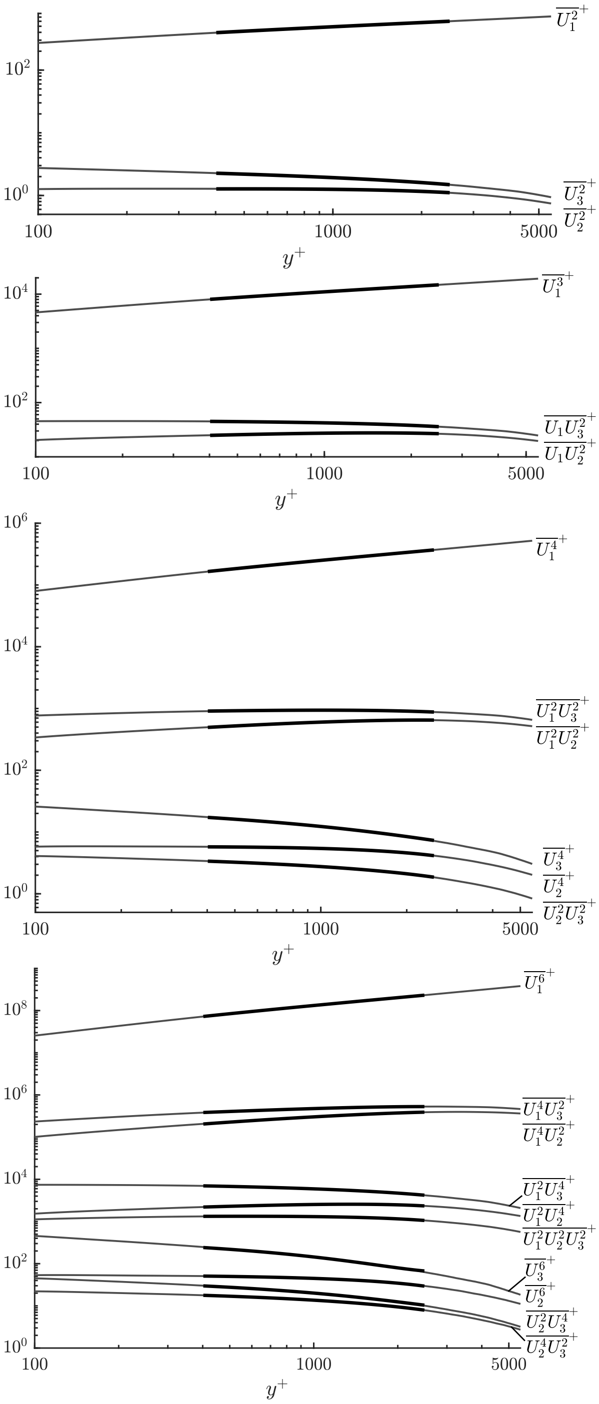

Figure 1: Velocity moments in the log region of order 2, 3, 4, and 6 from top to bottom. The thin gray lines represent the DNS data, and the thicker black lines correspond to formula (20). The legend on the right of each subfigure lists the specific moments $\overline{U_1^i U_2^j U_3^k}^+$. The corresponding integers i, j, k in the exponents may also become zero.

priori, i.e., $a^L = 0$, and we finally obtain

$$\mathcal{D}\overline{U_1^i U_2^j U_3^k}^+ = \frac{\left|\overline{U_1^i U_2^j U_3^k}^{(0)} - \overline{U_1^i U_2^j U_3^k}\right|}{u_\tau^n}$$
$$= C'_{[i,j,k]} \left(\frac{x_2}{h}\right)^{n(\sigma_2-\sigma_1)+2\sigma_1-\sigma_2}, \quad \text{with} \quad n = i+j+k. \quad (21)$$

Further, we define $\overline{U_1^i U_2^j U_3^k}^{(0)} = \overline{U_1^i U_2^j U_3^k}(x_2 = 0)$, and the absolute value in (21) was introduced solely to ensure that $C'_{[i,j,k]} > 0$ for all subsequent plots.

In the four subimages of figure 2, the DNS data in deficit form according to formula (21) are now plotted double-logarithmically sorted by specific moment orders. Although the error in comparison to the symmetry theory increases with growing moment order, it is very clear that the slopes for all moments are largely identical, i.e., the values from Oberlack *et al.* (2022), namely $\sigma_1 = 1.95$ and $\sigma_2 = 1.94$, are also reproduced here with high accuracy. Conversely, this means that the scaling exponents of all moments are independent of the moment order $n = i + j + k$. The error in the exponents for the high moments is only marginally higher than the 1% measured in Oberlack *et al.* (2022), and in general it can also be said that statistical convergence is worse in the center of the channel than in the log region.

An identical exponent for all moments, essentially based on $\sigma_1 \simeq \sigma_2$, implies strong anomalous scaling. So if we set $\sigma_1 = \sigma_2$ in (18), this leads to the following symmetry breaking

$$a_{Sx} = a_{St}. \tag{22}$$

i.e, the scaling of the instantaneous velocities in (5) is lost, while the scaling by the intermittency symmetry (10) due to a_{Ss} is preserved, and we find a common exponent for all moments of a_{Ss}/a_{Sx}. We recall that a_{Ss} is a measure of intermittent behaviour of turbulence. Hence, we have an initially unknown but *strongly intermittent* and *instantaneous* velocity scale in the channel center, i.e. an invariant, to which we assign the velocity scale u^*. To understand the invariant u^* more precisely, let us consider the ratio of any two moment deficits in (21), e.g., of $\bar{U}_1$ and $\overline{U_1^2}$, and we find the invariant

$$\frac{\overline{U_1^2}^{(0)} - \overline{U_1^2}}{\overline{U_1}^{(0)} - \overline{U_1}} = e^{\beta'} u_\tau. \tag{23}$$

The key finding here is that u_τ is also symmetry-breaking in the channel center, but the symmetry breakings in the log region in (14) and presently in (22) obviously have fundamentally different meanings and effects. Furthermore, Eq. (23) is always an invariant, regardless of which moments have been employed.

The logarithmic region (Fig. 1) and the deficit region (Fig. 2) both show that the moments containing U_1, and in some cases only these, take on very high numerical values. This clearly distinguishes them from the moments that are formed solely from the fluctuations, i. e. based on U_2 and U_3. In fact, however, only the parameters B and C assume high values (see Oberlack & Hoyas (2026)), because the exponents ω, σ_1, and σ_2 are identical in all cases. This primarily leads to a shift along the vertical axis, but the slopes are not affected.

There are two universal constants for each of the two regions, i.e., in the log region these are κ and ω, and in the channel center σ_1 and σ_2, whereby the latter are identical in principle, leaving only one constant. It seems sensible to anchor these properties in turbulence models, whereby κ is already embedded in virtually all models for model calibration. In fact, it proved extremely difficult to embed the statistical symmetries (9) and (10) in turbulence models, though an initial attempt can be found in Klingenberg *et al.* (2020).

5 SUMMERY AND CONCLUSION

Presently, we have shown that symmetry theory allows further deep insight into turbulence statistics for arbitrary sta-

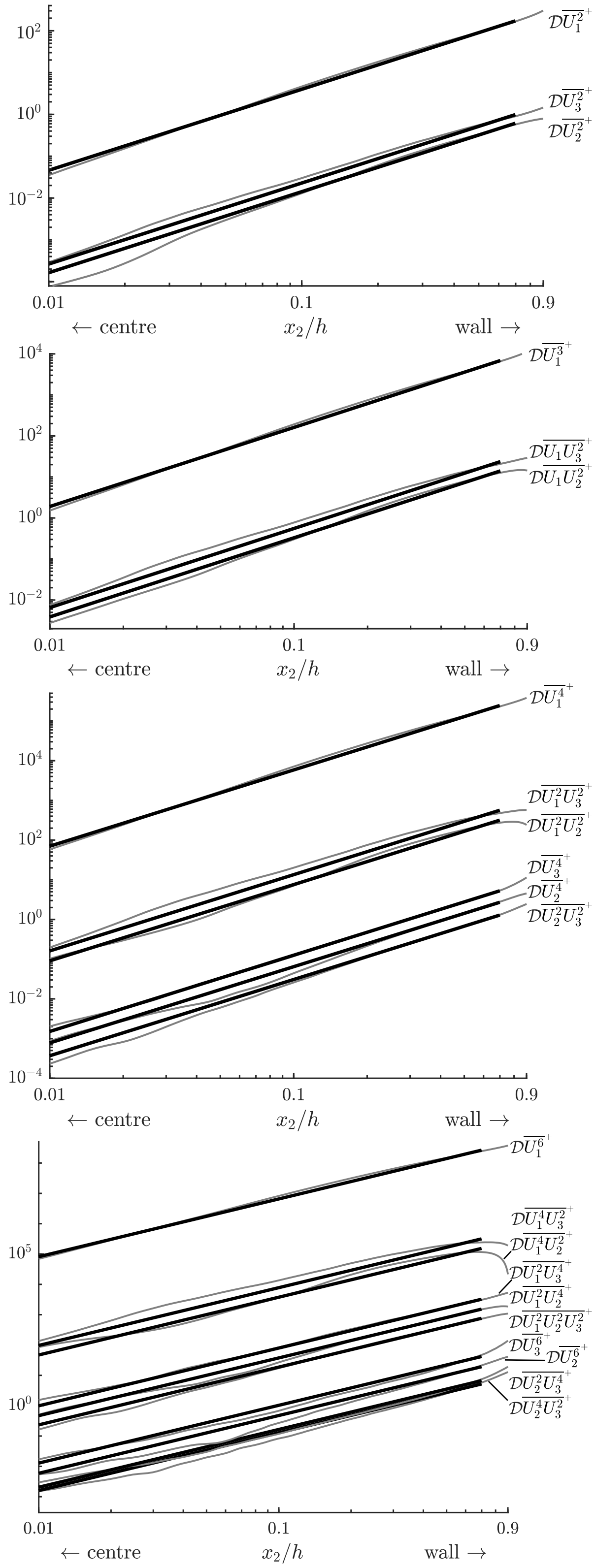

Figure 2: Velocity moments of order 2, 3, 4, and 6 from top to bottom in deficit form in the channel center region. The thin gray lines represent the DNS data, and the thicker black lines correspond to formula (21). The abbreviation for the deficit scaling on the right of each subfigure was introduced in (21).

tistical moments in wall-bound turbulence. A significant extension of the large-scale simulation with a sufficiently large Reynolds number was necessary to clearly demonstrate this in the logarithmic layer and a generalized deficit law in the center region of the channel. Two structural results distinguish the present analysis from the U_1-only treatment in Oberlack *et al.* (2022): (i) the same exponents ω, σ_1, σ_2 govern moments built from U_2 and U_3, which contain no mean velocity, removing the natural concern that the agreement in Oberlack *et al.* (2022) could be tied to the special role of $\overline{U}_1$; and (ii) in conjunction with Görtz *et al.* (2026), the scaling laws are shown to be invariant solutions of the infinite multi-point moment hierarchy in the precise Lie-group sense, i.e., the hierarchy reduces in the number of independent variables when the scaling laws are inserted – the same notion that, applied to the boundary-layer equations, produces the Blasius solution, but here for an infinite-dimensional system.

The authors gratefully acknowledge providing computing time on the Gauss Centre for Supercomputing e.V. on the GCS Supercomputer SuperMUC-NG at Leibniz Supercomputing Centre under project number pn49ya. SG and MO acknowledge funding by the Deutsche Forschungsgemeinschaft (DFG, German Research Foundation) - SPP 2410 Hyperbolic Balance Laws in Fluid Mechanics: Complexity, Scales, Randomness (CoScaRa), within the Project “Approximation Methods for Statistical Conservation Laws of Hyperbolically Dominated Flow” under project number 526024901.

References

Clauser, F. H. 1954 The turbulent boundary layer. *Advances in Applied Mechanics* **IV**, 1–51.

Coles, D. 1956 The law of the wake in the turbulent boundary layer. *Journal of Fluid Mechanics* **1**, 191–226.

George, W. K. 2006 Recent advancements toward the understanding of turbulent boundary layers. *AIAA Journal* **44**, 2435–2449.

Görtz, Simon, Conrad, Johannes & Oberlack, Martin 2026 High-moment scaling laws of wall-bounded turbulent shear flows: invariant solutions to the infinite multi-point moment equations. *under review with Phys. Rev. Fluids* .

Hoyas, Sergio, Oberlack, Martin, Alcántara-Ávila, Francisco, Kraheberger, Stefanie V. & Laux, Jonathan 2022 Wall turbulence at high friction reynolds numbers. *Phys. Rev. Fluids* **7**, 014602.

Isakson, A. 1937 On the formula for the velocity distribution near walls. *Technical Physics of the U.S.S.R.* **IV**, 155–162, no DOI available.

von Kármán, T. 1930 Mechanische Ähnlichkeit und Turbulenz. *Nachr. Ges. Wiss. Göttingen* **58-76**.

von Kármán, Theodore & Howarth, Leslie 1938 On the statistical theory of isotropic turbulence. *Proceedings of the Royal Society of London. Series A-Mathematical and Physical Sciences* **164** (917), 192–215.

Klewicki, J., Fife, P. & Wei, T. 2009 On the logarithmic mean profile. *Journal of Fluid Mechanics* **638**, 73–93.

Klingenberg, D., Plümacher, D. & Oberlack, M. 2020 Symmetries and turbulence modeling. *Phys. Fluids* **32**, 025108.

Kolmogorov, A. N. 1941 The local structure of turbulence in incompressible viscous fluid for very large Reynolds numbers. *Doklady Akademii Nauk SSSR* **30**, 301–305.

L. Keller & A. Friedmann 1924 Differentialgleichungen für die turbulente Bewegung einer kompressiblen Flüssigkeit. *Proc. First. Int. Congr. Appl. Mech. (Technische Boekhandel en Drukkerij, Delft, 1924)* pp. 395–405.

L. Prandtl 1932 Zur turbulenten Strömung in Rohren und längs Platten. *Ergeb. Aerod. Versuch Göttingen, IV Lieferung, 4.* pp. 395–405.

Lundgren, T. S. 2003 Kolmogorov turbulence by matched asymptotic expansions. *Physics of Fluids* **15** (4), 1074–1081.

Marusic, Ivan & Monty, Jason P. 2019 Attached eddy model of wall turbulence. *Annual Review of Fluid Mechanics* **51** (Volume 51, 2019), 49–74.

Millikan, C. B. 1938 A critical discussion of turbulent flows in channels and circular tubes. In *Proceedings of the 5th International Congress on Applied Mechanics* (ed. J. P. den Hartog & H. Peters), pp. 386–392. New York, NY; London, UK: John Wiley & Sons.

Oberlack, Martin 2001 A unified approach for symmetries in plane parallel turbulent shear flows. *Journal of Fluid Mechanics* **427**, 299–328.

Oberlack, M. & Hoyas, S. 2026 Extended DNS data base of a turbulent channel flow at $Re_\tau = 10000$.

Oberlack, Martin, Hoyas, Sergio, Kraheberger, Stefanie V., Alcántara-Ávila, Francisco & Laux, Jonathan 2022 Turbulence statistics of arbitrary moments of wall-bounded shear flows: A symmetry approach. *Phys. Rev. Lett.* **128**, 024502.

Oberlack, Martin & Peters, Norbert 1993 *Closure of the Two-Point Correlation Equation in Physical Space as a Basis for Reynolds Stress Models*, pp. 85–94. Elsevier Science.

Oberlack, Martin & Rosteck, Andreas 2010 New statistical symmetries of the multi-point equations and its importance for turbulent scaling laws. *Discrete Continuous Dyn. Syst* **3**, 451–471.

Reynolds, Osborne 1895 On the dynamical theory of incompressible viscous fluids and the determination of the criterion. *Philosophical Transactions of the Royal Society of London, Series A* **186**, 123–164.

Rosteck, Andreas 2013 Scaling laws in turbulence - a theoretical approach using lie-point symmetries. PhD thesis, Technische Universität Darmstadt.

Spalart, Philippe R. & Abe, Hiroyuki 2021 Empirical scaling laws for wall-bounded turbulence deduced from direct numerical simulations. *Phys. Rev. Fluids* **6**, 044604.

Townsend, A. A. 1976 *The Structure of Turbulent Shear Flow*, 2nd edn. *Cambridge Monographs on Mechanics and Applied Mathematics*. Cambridge: Cambridge University Press.

Wacławczyk, Marta, Staffolani, Nicola, Oberlack, Martin, Rosteck, Andreas, Wilczek, Michael & Friedrich, Rudolf 2014 Statistical symmetries of the Lundgren-Monin-Novikov hierarchy. *Physical Review E* **90** (1), 013022.

Örlü, R., Fiorini, T., Segalini, A., Bellani, G., Talamelli, A. & Alfredsson, P. H. 2017 Reynolds stress scaling in pipe flow turbulence—first results from ciclope. *Philosophical Transactions of the Royal Society A: Mathematical, Physical and Engineering Sciences* **375** (2089), 20160187.